BNL-211727-2019-JAAM

Modulating Carrier Transport via Defect Engineering in Solar Water Splitting Devices

W. Zhang, M. Liu

To be published in "ACS Energy Letters"

March 2019

Center for Functional Nanomaterials

Brookhaven National Laboratory

U.S. Department of Energy

USDOE Office of Science (SC), Basic Energy Sciences (BES) (SC-22)

Notice: This manuscript has been authored by employees of Brookhaven Science Associates, LLC under Contract No. DE-SC0012704 with the U.S. Department of Energy. The publisher by accepting the manuscript for publication acknowledges that the United States Government retains a non-exclusive, paid-up, irrevocable, world-wide license to publish or reproduce the published form of this manuscript, or allow others to do so, for United States Government purposes.

DISCLAIMER

This report was prepared as an account of work sponsored by an agency of the United States Government. Neither the United States Government nor any agency thereof, nor any of their employees, nor any of their contractors, subcontractors, or their employees, makes any warranty, express or implied, or assumes any legal liability or responsibility for the accuracy, completeness, or any third party's use or the results of such use of any information, apparatus, product, or process disclosed, or represents that its use would not infringe privately owned rights. Reference herein to any specific commercial product, process, or service by trade name, trademark, manufacturer, or otherwise, does not necessarily constitute or imply its endorsement, recommendation, or favoring by the United States Government or any agency thereof or its contractors or subcontractors. The views and opinions of authors expressed herein do not necessarily state or reflect those of the United States Government or any agency thereof.

Modulating Carrier Transport via Defect Engineering in Solar Water Splitting Devices

Wenrui Zhang* and Mingzhao Liu*

Center for Functional Nanomaterials, Brookhaven National Laboratory, Upton, New York 11973, USA

ABSTRACT

Developing sustainable solar water splitting devices requires efficient separation and transport of photogenerated carriers. In this perspective, we examine carrier transport in semiconductor photoelectrodes using bismuth vanadate as a primary model system and highlight strategies to significantly improve carrier delivery through defect engineering. To improve electron transport in low mobility semiconductors, we introduce two distinct bulk doping methods, by homogenously enhancing the bulk defect level or by forming distributed homojunctions with graded doping. Next, we demonstrate the use of structural boundaries as extrinsic pathways for fast electron transport, thus providing novel insights to engineer materials' macroscopic conductivity. Third, we describe the importance of interface design in terms of structural, chemical, and electronic matching at the back contact to suppress carrier recombination. Finally, we highlight the methods for surface defect control via passivation and catalysis, and give a brief outlook of research challenges and opportunities for solar water splitting.

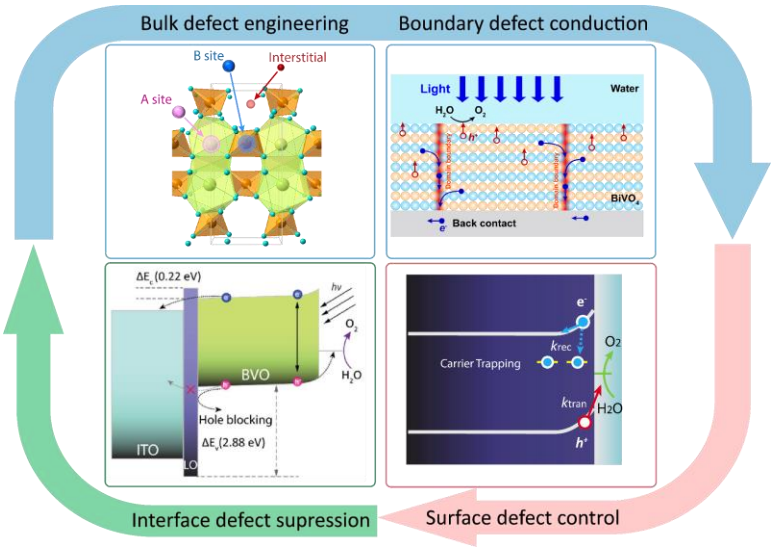

(TOC graphic)

Owing to their superior energy density and portability, a viable solution to replace chemical fuels at a substantial scale remains elusive, despite the imminent arrival of the global climate change tipping point.[1,2] Harvesting solar energy for chemical fuel production would fulfill the demand of human society without negative climate impact. A promising route to produce solar fuel is based on photoelectrochemical (PEC) reactions, which captures solar energy and converts it to free energy in chemical bonds of hydrogen or carbon-based fuels (Figure 1a).[3-5] In typical PEC cells, semiconductor photoelectrodes absorb incident photons to generate electron-hole pairs, which are separated and delivered to cathode surface for reduction reaction and to anode surface for oxidation reaction, respectively. The material requirements to make an efficient photoelectrode are demanding.[6-8] The semiconductor should possess appropriate band gaps for strong visible light absorption and should have band edges positioned preferably for redox reactions. The semiconductor should also support fast charge carrier separation and transport, and form a chemically stable surface with decent catalytic activity. The requirements become even more stringent for photoanodes used for PEC water oxidation, which involves multiple electron/proton transfer and is kinetically more sluggish.[9,10] Since the first water photolysis work by Fujishima and Honda,[11] significant research efforts have been devoted in identifying low-cost and highly-efficient photoanode materials, which include binary metal oxides (TiO_2,[12] ZnO,[13] α-Fe_2O_3,[14] WO_3[15]), complex oxides (perovskite $SrTiO_3$,[16] $BiVO_4$ (BVO)[17]), and nitrides (Ta_3N_5,[18] InGaN[19]). However, no single material has yet simultaneously satisfied all the requirements to make an economically sustainable device for solar fuel production.

Current approaches to accelerating the semiconductor photoelectrode development include high-throughput materials synthesis and screening, hybrid system integration for multispectral light absorption and/or carrier separation, materials modification from structural and chemical

engineering. Encouraging progress has been made in synthesizing narrow-gap materials guided by computational design, [20] constructing tandem devices,[21] exploring doping and nanostructuring, [22] and developing conformal surface catalyst.[23] Beside those topics, carrier transport in semiconductor photoelectrodes is a key process that determines the PEC device efficiency and is extremely sensitive to the materials defect level. In this perspective, we focus on carrier transport in semiconductors and highlight strategies to improve it via defect engineering. We start with a brief introduction of the fundamental process of carrier transport in a working photoelectrode. Following that, we discuss the strategies to improve carrier separation and transport by introducing four types of defects, which include *bulk* defect, structural boundary defect, interface defect at the back contact, and aqueous surface defect. An outlook of future work is presented in the final section. By establishing the relation between defect and carrier transport, novel mechanistic understandings and coordinated semiconductor design strategies are expected to assist the fabrication of low-cost and highly-efficient solar water splitting devices.

***Carrier transport in semiconductor photoelectrod*es.** The PEC device performance is determined by the light absorption efficiency and the carrier delivery efficiency. Therefore, coordinating carrier transport with light absorption is essential to maximize the energy conversion efficiency of semiconductor photoelectrodes. For a given semiconductor, the light absorption is fundamentally determined by its band structure, through two common descriptors: the band gap and the optical absorption coefficient (α). The latter determines the effective photon attenuation depth, $d_p = 1/\alpha$, which describes the material depth required for efficient photocarrier generation (Figure 1b). Upon generation, photocarriers must be extracted from the photoelectrode for PEC reactions, which is inevitably accompanied by carrier recombination. Depending on the specific role during carrier transport process, the photoelectrode can be divided in to three regions, which

are the semiconductor bulk, the semiconductor/back contact interface, and the aqueous surface. Suppressing carrier recombination in those three regions becomes the key to improving the PEC device efficiency.

The semiconductor bulk can be further divided into two neighboring regions: the space charge region (SCR) and the adjacent quasi-neutral region, and is responsible for the majority of photocarrier generation and transport. The photocarrier transport across the SCR, as described by the SCR width (d_{sc}), is usually more efficient due to the built-in electric field. In the quasi-neutral region, photocarrier transport is dominated by diffusion and is generally more vulnerable to recombination. The minority carrier diffusion length (d_h) determines how far the photocarriers in this neutral region can travel. In general, the sum of d_h and d_{sc} should be no smaller than d_p, so that the photoelectrode achieves maximized energy conversion from absorbed photons to photocarriers for PEC reactions. This serves as a basic design guideline to engineer semiconductors for PEC water splitting in classical carrier transport models.[24-26]

Bulk defect with uniform doping. For low-mobility semiconductors, the concentration of ionized bulk defects that are located near the band edges determines the carrier transport efficiency. Engineering the bulk defect level becomes extremely important for optimized carrier delivery. This is observed in state-of-the-art oxygen evolving photoanodes, including those of $BiVO_4$ (BVO)[27] and α-Fe_2O_3.[28] As a complex oxide (ternary ABO_x), BVO allows three sites for bulk doping to improve the overall transport performance (Figure 2a). This includes A-site doping with Ce,[29] B-site doping with tungsten (W) or molybdenum (Mo),[30] and interstitial site doping with hydrogen donors.[31-33] In general, the mechanism for A- or B- site doping is to improve the electron density via incorporating extrinsic high-valence donors uniformly in the bulk. In particular,

substituting Mo or W into the vanadium sites have been widely used to improve the electrode conductivity and PEC activity in BVO.[27,30]

On the other hand, introducing hydrogen defects through mild annealing treatments also effectively improve the BVO PEC performance.[31-33] This treatment was initially proposed to generate more oxygen vacancies, which serve as shallow donors to increase the BVO conductivity and PEC activity.[31] More recently, it was suggested that the hydrogen treatment may play a fundamentally different role in tuning the carrier transport.[32] The hydrogen impurity can readily diffuse within the BVO lattice and stabilize as interstitial donors. According to time-resolved microwave conductivity measurements by Jang et al (Figure 2b),[33] these hydrogen donors were suggested to effectively improve the minority carrier lifetime, rather than enhancing the majority carrier density as the W or Mo doping usually does. Although the uniform bulk doping using hydrogen or hexavalent ions apparently improves the PEC performance, the fundamental mechanism has yet to be fully elucidated. For example, while the hydrogen annealing can enhance the level of hydrogen impurities, it may also generate more oxygen vacancies. Hydrogen intercalation is also known to be effective in passivating dangling bonds and removing deep-level defects, which may help improve carrier transport in semiconductors.[34,35] Discrepancies exist in identifying which type of defect dominates the carrier transport in BVO, generating pressing needs for further computational and experimental efforts.

(Subsection) Unconventional transport with small polaron hopping. While it is well recognized that W or Mo doping should increase the majority carrier density, they have other, nontrivial impact on the majority carrier mobility and the minority carrier transport. To assess the dopant role in modulating carrier transport, including both carrier density and minority, we examined a model system of Mo-doped $BiVO_4$ (Mo-BVO) using a single-crystalline thin film

approach. It is straightforward to understand the relation between Mo doping and the electron density, but its relation with the electron mobility is more obscure, as the value is beyond the detection limit for conventional evaluation methods. The low electron mobility in BVO arises from the formation of small polaron, due to short-range interaction with neighboring lattice vibrations.[36,37] To complete an electron transfer, the local lattice distortion accompanied with the electron is also transferred, possessing an activation energy or hopping barrier (E_a) (Figure 3a). Near room temperature, the hopping rate follows an Arrhenius temperature dependence, and the *dc* conductivity ($\sigma(T)$) may be described by

$$\sigma(T) = AT^{-1} \exp\left(\frac{-E_a}{k_B T}\right), \quad (1)$$

where A is a prefactor and k_B the Boltzmann constant.[37]

The successful development of single-crystalline Mo-BVO thin films enabled us to confirm whether extrinsic doping affects the electron mobility and evaluated its impact on the PEC performance (Figure 3b).[38] Interestingly, the Mo doping not only increases the electron density, but also improves the electron mobility, as suggested by the much reduced E_a in Mo-BVO films (Figure 3c). Meanwhile, the Mo doping slightly reduces the hole diffusion length, as the higher donor density enhances the chance of hole recombination. This synergic effect has profound impact on the water oxidation photocurrents: Mo-BVO photoanodes deliver larger photocurrents than pristine BVO at a thickness less than one-third of the pristine BVO film (Figure 3d). This finding complements classical transport models, which assume the majority carrier transport is not a limiting factor, but mainly concerns the minority carrier transport and light absorption. These results, however, demonstrate the importance of overcoming the majority carrier transport limitation in improving the PEC performance in low-mobility semiconductors.

Bulk defect with graded doping. Instead of introducing a homogeneous spatial profile of dopants, graded doping artificially constructs a sloped or stepped distribution of the doping level to form distributed homo-junctions. This provides a novel way to enhance charge carrier transport for low-mobility semiconductors. When a heavily *n*-doped semiconductor comes into contact with a lightly doped one of the same kind, a n^+-*n* homojunction forms across the interface and generates a built-in electric field that assists the carrier separation and transport. The graded doping strategy maximizes the homojunction function and enables superior carrier transport over a much longer distance beyond SCR. This effect was demonstrated by a systematic comparison between different types of W-doped BVO/BVO homojunctions (Figure 4a) in the work of Abdi et al.[39] A graded W-doped BVO photoanode was constructed with ten stepped concentration gradients from 1% W at the back contact to 0% at the top surface. This graded doping strategy largely enhances the charge separation efficiency to 60%, representing a 58% increase over the homogeneously W-doped BVO (Figure 4b).

The graded doping strategy is also helpful to match d_{sc} with d_p for optimized PEC performance in other material systems. This is particularly important for indirect-gap semiconductors, where d_p is usually much larger than the sum of d_h and d_{sc} due to the weak optical absorption. For example, $SrTiO_3$ has an indirect gap at 3.25 eV and is capable to drive overall water splitting at zero bias.[40,41] However, the optical absorption for indirect transitions is very weak ($\alpha < 10^4$ cm^{-1} at 3.25 eV), which requires a d_p (>1000 nm) that is far beyond its d_h (~10 nm).[42] To address this problem, we applied the graded doping strategy to significantly widen d_{sc} for matching d_p.[16] Through an initial vacuum annealing and a following partial oxygen vacancy replenishing (Figure 4c), we obtained an *n*-$SrTiO_3$ photoanode with heavy doping in the bulk for high electron conductivity but light doping at the surface for larger d_{sc} over 500 nm (Figure 4d). As a result, the graded *n*-$SrTiO_3$

photoanode achieves greatly enhanced incident photon to electron (IPCE) efficiency for indirect band gap excitation (Figure 4e).

Domain boundary conduction assisted by boundary defect. Beside tuning the intrinsic materials characteristics with bulk defect, engineering extrinsic structural imperfections, such as mobile charged defects at boundaries, is effective to improve carrier transport. In this section, we highlight the efforts to work with domain boundary defects for improved carrier transport and PEC activity. In thin films or nanostructures, domain or grain boundaries vastly exist during materials growth and processing. Although these defects are actively involved in the macroscopic carrier transport, their impact on semiconductor photoelectrode performance is less understood. To study the boundary effect on carrier transport, we fabricated *c*-axis oriented BVO thin films that feature a high density of continuous, vertical interfaces that arise from in-plane domain rotation.[43] These domain boundaries serve as fast transport channels for electrons diffusing into this region, and therefore enhance the macroscopic out-of-plane conductivity (Figure 5a). Solid-state electronic characterizations revealed that the multi-domain BVO film exhibits anomalously high out-of-plane conductivity, which is nearly four orders of magnitude larger than the characteristic intrinsic conductivity. The extra conductivity offered by domain boundaries was further identified by conductive atomic force microscopy (AFM) measurements on multi-domain BVO (Figure 5b, c).

In a further development, Eichhorn et al integrated conductive AFM with optical excitation to polycrystalline BVO, which enabled the investigation of charge transport mechanism involving photoelectrons (Figure 5d).[44] The domain boundary conduction was also observed in this study. The limitation of charge carrier transport inside BVO was further studied through a systematic temperature and illumination intensity dependent study. Regardless of the AFM tip coating, a power law dependence is observed from the linear log(J)-log(V) (*current-voltage*) relations at high

biases (Figure 5e), reflecting a space-charge limited regime with trap state contributions.[45] This study directly mapped the photoconductivity inhomogeneity from various structural features, including grains, boundaries, and crystal facts in polycrystalline BVO films, and identified the mechanism of charge transport limitation in BVO. The emerging conductivity at structural boundaries has profound impact on the photocarrier transport and photoelectrode design. Photoelectrons can take the vertical domain boundaries as a least action path to back contact, instead of moving slowly inside domains and getting recombined. In this way, it compensates the intrinsic low electron transport. This finding also presents a new design strategy that one can work with domain width and distribution to match the photocarrier diffusion length, so that the macroscopic carrier transport can be tuned by extrinsic structural variables.

Suppress boundary recombination with hole-blocking interface. Once photocarriers leave the semiconductor bulk, they are collected at the back contact or the aqueous surface. However, severe carrier recombination can occur at these interfaces due to the abundance of defects and dangling bonds. For example, a "dead layer" often forms near the back contact due to imperfect lattice alignment or chemical interdiffusion.[46-48] To facilitate carrier transfer across the back contact, careful interface design is required in terms of structural, chemical and electronic matching. The importance of interface design is demonstrated in a recent study on BVO thin film photoanodes, which prefer back-illumination for larger photocurrent, due to the sluggish electron transport.[27] However, this configuration inevitably exposes photoholes to recombination centers at the back contact. To suppress such recombination, we introduced a lutetium oxide (Lu_2O_3) interlayer between the bottom indium tin oxide (ITO) layer and the upper BVO film.[49] The Lu_2O_3 interlayer facilitates epitaxial growth of BVO, which minimizes the structural defect formation at the interface (Figure 6a). Meanwhile, as a wide band gap semiconductor (E_g = 5.7 eV), Lu_2O_3 forms

a unique band alignment with BVO that is efficient for hole blocking (ΔE_v = 2.88 eV), but feasible for electron tunneling (ΔE_c = 0.22 eV) (Figure 6b). As a result, an ultrathin Lu_2O_3 layer (1.4-nm-thick) significantly improves the charge separation efficiency in BVO and correspondingly the water splitting activity (Figure 6c).

Surface defect engineering via passivation and catalysis. For carriers delivered to the electrolyte interface, surface recombination can be a significant loss channel when the surface defect level is high or when the chemical reaction rate is slow (Figure 7a), as seen in the exemplary α-Fe_2O_3[50] and BVO photoanodes.[51] To minimize surface recombination, two closely related strategies are usually exploited: passivating the surface defect and capping a catalyst overlayer.[52] Rate constant analysis is usually used to distinguish these two effects, which can be obtained from intensity modulated photocurrent spectroscopy measurements. For example, Jang et al applied a hydrothermal regrowth method to α-Fe_2O_3 photoanodes to reduce the surface defect density, which readily reduces the photocurrent onset potential (E_{onset}) from the usual 1.07 V_{RHE} to 0.67 V_{RHE}.[50] The carrier transport at the surface is further improved by coating an amorphous $NiFeO_x$ layer, which reduces the E_{onset} to 0.45 V_{RHE}. However, this surface layer does not improve the charge transfer rate constant (k_{tran}).[53] Instead, both the regrowth method and the $NiFeO_x$ surface layer passivate surface defects to suppress carrier recombination, resulting in significantly improved charge transfer efficiency (Figure 7b). Due to the reduced carrier recombination constant (k_{rec}), both the surface hole concentration and the photovoltage are improved, leading to much lower E_{onset}. In comparison with surface defect passivation that mainly enhances k_{rec}, a surface catalysis layer improves the chemical reaction rate, which is featured by larger k_{tran} at the catalyst/electrolyte interface (Figure 7c). This was demonstrated by Kim et al, where a serial dual-layer FeOOH/NiOOH surface catalyst alters the water-splitting chemistry on the BVO surface and

significantly enhances the charge carrier separation.[17] It should be also noted that the catalysis effect can work together with the defect passivation effect for a range of heterogeneous catalysts, such as cobalt phosphate (Co-Pi) and IrO_x.[54,55] To date, the mechanism of specific catalyst function remains under intense investigation. In various cases, apparently contradictory answers may be drawn from different techniques on the same catalyst. For example, a "dual-working-electrode" technique directly probes the charge carrier passing through the coated photoelectrodes,[56] and detects catalytic effects from $NiFeO_x$ overlayers for α-Fe_2O_3 photoanodes that are considered as passivation layers by other techniques.[53,57]

Identify the origin of carrier transport limitation. We have highlighted recent research efforts to improve carrier transport by engineering defects in different regions across semiconductor photoelectrodes. For exploratory device optimization, it is critical to first pinpoint the origin of carrier transport limitation and then apply defect engineering strategies accordingly. Conventional PEC measurements are most commonly used. Comparing photocurrents from water oxidation and hole scavenger oxidation gives a convenient estimation of charge separation efficiency of the photoelectrode.[17,51] Probing the illumination dependence of photocurrent is an effective way to qualitatively determine whether the carrier transport in limited by majority or minority charge carriers. Meanwhile, directly tracking carrier transport via *I-V* measurements is another important way to understand the transport mechanism and limitation.[38,43,58] This approach includes macroscopic resistivity measurements in a thin film capacitor geometry and microscopic measurements using conductive atomic force microscope. The latter one can be further modified with optical excitation in electrolyte for operando transport characterizations.[44,59] In addition, optical pump-probe spectroscopy and impedance spectroscopy are effective to pinpoint the limiting factors for carrier relaxation across different time scales and spatial regions.[53,60-62]

Summary and outlook. We have discussed defect engineering strategies to facilitate charge carrier transport and to coordinate with light absorption for optimized energy conversion efficiency. These defect engineering strategies are not isolated from each other and may work together to improve the photoelectrode performance. So far, the best material candidate that is commercially competitive for solar energy conversion is yet to be identified. To accelerate materials design and discovery in the field, further research efforts are proposed as follows:

(1) Mechanism and application of defect engineering. As we have discussed in this work, the impact of defect on carrier transport can be complicated and non-trivial: defects can be detrimental as recombination centers, but they can also be beneficial as carrier donors. For example, in the model system of BVO, native defects such as oxygen vacancies, start to enhance the macroscopic film conductivity only at relatively high deposition temperatures (600 ℃).[43] Such film conductivity, however, is not observed for films deposited at medium temperatures (350 ℃- 400 ℃).[63] Beyond carrier transport, incorporating defects may simultaneously alter the optical transitions and so the light absorption, such as hydrogenated TiO_2[64] and nitrogen-intercalated WO_3.[65] Therefore, elucidating the defect mechanism and activating the desired function are critical to boost the photoelectrode performance, and require further theoretical and experimental efforts.

(2) Operando characterization. Probing charge carrier dynamics at operando conditions provides critical insights that are not accessible by conventional solid-state carrier transport and steady-state PEC characterizations. Optical pump-probe spectroscopy and impedance spectroscopy have been integrated with a working photoelectrode to probe the carrier relaxation process across different time scales and spatial regions.[53,60-62] Furthermore, when coupling carrier dynamics measurements with structural/chemical characterizations, a full structure-property relation can be established, which is extremely important to drive materials design. Current operando techniques for

monitoring the chemical, structural and morphological evolution at working conditions includes X-ray photoemission spectroscopy for energetics evolution at the aqueous interface,[66] infrared absorption for surface intermediates absorption,[67] X-ray absorption spectroscopy for bulk electronic and lattice structure,[68] and electrochemical AFM for surface morphology evolution.[69]

(3) Exploratory material design. Transforming mechanistic understanding to novel materials development is significant to obtain ultimate high-performance and low-cost photoelectrodes. It is important to expand current materials selection from oxides to non-oxides, such as nitrides and oxynitrides (Ta_3N_5,[18] InGaN,[19] TaON,[70] GaN-ZnO[71]), sulfides and phosphides.[72] Although the latter materials generally absorb more visible light absorption, they suffer from surface corrosion and carrier recombination. Therefore, it is critical to transform the insights that we gained from oxide systems to non-oxide systems in order to improve their PEC performance. Another promising direction is high-throughput materials computation and synthesis. The computation methodology development accelerates materials discovery in the ternary or even more complex regime.[20,73,74] This prolific approach exploits the key relations between structural motifs and electronic/optical transitions for materials screening. These calculation findings can guide the material synthesis and characterization efforts, which, in turn, provides experimental feedback to the calculations. This integrated theory-experiment loop is expected to play an increasing role in searching promising semiconductors for solar energy conversion.

AUTHOR INFORMATION

Corresponding Author

*E-mail: zhwrican@gmail.com

*E-mail: mzliu@bnl.gov

Notes

The authors declare no competing financial interest.

Biographies

Wenrui Zhang is a Research Associate at Brookhaven National Laboratory, where his research focuses on semiconductor thin film synthesis and carrier transport mechanism for solar fuel production. He received his Ph.D. in Materials Science and Engineering from Texas A&M University in 2015.

Mingzhao Liu is a Materials Scientist in Center for Functional Nanomaterials at Brookhaven National Laboratory. His research group studies vapor phase synthesis of thin film materials for applications in solar fuel conversion. He received his Ph.D. in Chemistry from The University of Chicago in 2007.

ACKNOWLEDGMENTS

This research used resources of the Center for Functional Nanomaterials, which is a U.S. DOE Office of Science User Facility, at Brookhaven National Laboratory under Contract No. DE-SC0012704.

REFERENCE

(1) Cox, P. M.; Huntingford, C.; Williamson, M. S. Emergent Constraint on Equilibrium Climate Sensitivity from Global Temperature Variability. *Nature* **2018,** *553*, 319.

(2) York, R. Do Alternative Energy Sources Displace Fossil Fuels? *Nat. Clim. Change* **2012,** *2*, 441.

(3) Lewis, N. S. Research Opportunities to Advance Solar Energy Utilization. *Science* **2016,** *351*.

(4) Montoya, J. H.; Seitz, L. C.; Chakthranont, P.; Vojvodic, A.; Jaramillo, T. F.; Nørskov, J. K. Materials for Solar Fuels and Chemicals. *Nat. Mater*. **2016,** *16*, 70.

(5) Tachibana, Y.; Vayssieres, L.; Durrant, J. R. Artificial Photosynthesis for Solar Water-Splitting. *Nat. Photon.* **2012,** *6*, 511-518.

(6) Walter, M. G.; Warren, E. L.; McKone, J. R.; Boettcher, S. W.; Mi, Q.; Santori, E. A.; Lewis, N. S. Solar Water Splitting Cells. *Chem. Rev.* **2010,** *110*, 6446-6473.

(7) Sivula, K.; van de Krol, R. Semiconducting Materials for Photoelectrochemical Energy Conversion. *Nat. Rev. Mater.* **2016,** *1*, 15010.

(8) Sharp, I. D.; Cooper, J. K.; Toma, F. M.; Buonsanti, R. Bismuth Vanadate as a Platform for Accelerating Discovery and Development of Complex Transition-Metal Oxide Photoanodes. *ACS Energy Lett.* **2017,** *2*, 139-150.

(9) Hisatomi, T.; Kubota, J.; Domen, K. Recent Advances in Semiconductors for Photocatalytic and Photoelectrochemical Water Splitting. *Chem. Soc. Rev.* **2014,** *43*, 7520-7535.

(10) Bhatt, M. D.; Lee, J. S. Recent Theoretical Progress in the Development of Photoanode Materials for Solar Water Splitting Photoelectrochemical Cells. *J. Mater. Chem. A* **2015,** *3*, 10632-10659.

(11) Fujishima, A.; Honda, K. Electrochemical Photolysis of Water at a Semiconductor Electrode. *Nature* **1972,** *238*, 37-38.

(12) Tang, J.; Durrant, J. R.; Klug, D. R. Mechanism of Photocatalytic Water Splitting in TiO_2. Reaction of Water with Photoholes, Importance of Charge Carrier Dynamics, and Evidence for Four-Hole Chemistry. *J. Am. Chem. Soc.* **2008,** *130*, 13885-13891.

(13) Zhang, W.; Yan, D.; Appavoo, K.; Cen, J.; Wu, Q.; Orlov, A.; Sfeir, M. Y.; Liu, M. Unravelling Photocarrier Dynamics Beyond the Space Charge Region for Photoelectrochemical Water Splitting. *Chem. Mater.* **2017,** *29*, 4036-4043.

(14) Grave, D. A.; Yatom, N.; Ellis, D. S.; Toroker, M. C.; Rothschild, A. The "Rust" Challenge: On the Correlations between Electronic Structure, Excited State Dynamics, and Photoelectrochemical Performance of Hematite Photoanodes for Solar Water Splitting. *Adv. Mater.* **2018,** *30*, 1706577.

(15) Liu, R.; Lin, Y.; Chou, L.-Y.; Sheehan, S. W.; He, W.; Zhang, F.; Hou, H. J. M.; Wang, D. Water Splitting by Tungsten Oxide Prepared by Atomic Layer Deposition and Decorated with an Oxygen-Evolving Catalyst. *Angew. Chem. Int. Ed.* **2011,** *50*, 499-502.

(16) Liu, M.; Lyons, J. L.; Yan, D.; Hybertsen, M. S. Semiconductor-Based Photoelectrochemical Water Splitting at the Limit of Very Wide Depletion Region. *Adv. Funct. Mater.* **2016,** *26*, 219-225.

(17) Kim, T. W.; Choi, K.-S. Nanoporous $BiVO_4$ Photoanodes with Dual-Layer Oxygen Evolution Catalysts for Solar Water Splitting. *Science* **2014,** *343*, 990-994.

(18) Li, Y.; Takata, T.; Cha, D.; Takanabe, K.; Minegishi, T.; Kubota, J.; Domen, K. Vertically Aligned Ta_3N_5 Nanorod Arrays for Solar-Driven Photoelectrochemical Water Splitting. *Adv. Mater.* **2013,** *25*, 125-131.

(19) Chu, S.; Vanka, S.; Wang, Y.; Gim, J.; Wang, Y.; Ra, Y.-H.; Hovden, R.; Guo, H.; Shih, I.; Mi, Z. Solar Water Oxidation by an InGaN Nanowire Photoanode with a Bandgap of 1.7 eV. *ACS Energy Lett.* **2018,** *3*, 307-314.

(20) Yan, Q.; Yu, J.; Suram, S. K.; Zhou, L.; Shinde, A.; Newhouse, P. F.; Chen, W.; Li, G.; Persson, K. A.; Gregoire, J. M. et al. Solar Fuels Photoanode Materials Discovery by Integrating High-Throughput Theory and Experiment. *Proc. Natl. Acad. Sci. USA* **2017,** *114*, 3040-3043.

(21) Zhang, K.; Ma, M.; Li, P.; Wang, D. H.; Park, J. H. Water Splitting Progress in Tandem Devices: Moving Photolysis Beyond Electrolysis. *Adv. Energy Mater.* **2016,** *6*, 1600602.

(22) Li, C.; Luo, Z.; Wang, T.; Gong, J. Surface, Bulk, and Interface: Rational Design of Hematite Architecture toward Efficient Photo-electrochemical Water Splitting. *Adv. Mater.* **2018,** *30*, 1707502.

(23) Roger, I.; Shipman, M. A.; Symes, M. D. Earth-Abundant Catalysts for Electrochemical and Photoelectrochemical Water Splitting. *Nat. Rev. Chem.* **2017,** *1*, 0003.

(24) Gärtner, W. W. Depletion-Layer Photoeffects in Semiconductors. *Phys. Rev.* **1959,** *116*, 84-87.

(25) Reichman, J. The Current-Voltage Characteristics of Semiconductor-Electrolyte Junction Photovoltaic Cells. *Appl. Phys. Lett.* **1980,** *36*, 574-577.

(26) Butler, M. A.; Ginley, D. S. Principles of Photoelectrochemical, Solar Energy Conversion. *J. Mater. Sci.* **1980,** *15*, 1-19.

(27) Park, Y.; McDonald, K. J.; Choi, K.-S. Progress in Bismuth Vanadate Photoanodes for Use in Solar Water Oxidation. *Chem. Soc. Rev.* **2013,** *42*, 2321-2337.

(28) Sivula, K.; Le Formal, F.; Grätzel, M. Solar Water Splitting: Progress Using Hematite (α-Fe_2O_3) Photoelectrodes. *ChemSusChem* **2011,** *4*, 432-449.

(29) Zhou, D.; Pang, L.-X.; Guo, J.; Qi, Z.-M.; Shao, T.; Wang, Q.-P.; Xie, H.-D.; Yao, X.; Randall, C. A. Influence of Ce Substitution for Bi in $BiVO_4$ and the Impact on the Phase Evolution and Microwave Dielectric Properties. *Inorg. Chem.* **2014,** *53*, 1048-1055.

(30) Park, H. S.; Kweon, K. E.; Ye, H.; Paek, E.; Hwang, G. S.; Bard, A. J. Factors in the Metal Doping of $BiVO_4$ for Improved Photoelectrocatalytic Activity as Studied by Scanning Electrochemical Microscopy and First-Principles Density-Functional Calculation. *J. Phys. Chem. C* **2011,** *115*, 17870-17879.

(31) Wang, G.; Ling, Y.; Lu, X.; Qian, F.; Tong, Y.; Zhang, J. Z.; Lordi, V.; Rocha Leao, C.; Li, Y. Computational and Photoelectrochemical Study of Hydrogenated Bismuth Vanadate. *J. Phys. Chem. C* **2013,** *117*, 10957-10964.

(32) Cooper, J. K.; Scott, S. B.; Ling, Y.; Yang, J.; Hao, S.; Li, Y.; Toma, F. M.; Stutzmann, M.; Lakshmi, K. V.; Sharp, I. D. Role of Hydrogen in Defining the N-Type Character of $BiVO_4$ Photoanodes. *Chem. Mater.* **2016,** *28*, 5761-5771.

(33) Jang, J.-W.; Friedrich, D.; Müller, S.; Lamers, M.; Hempel, H.; Lardhi, S.; Cao, Z.; Harb, M.; Cavallo, L.; Heller, R. et al. Enhancing Charge Carrier Lifetime in Metal Oxide Photoelectrodes through Mild Hydrogen Treatment. *Adv. Energy Mater.* **2017,** *7*, 1701536.

(34) Martinuzzi, S.; Périchaud, I.; Warchol, F. Hydrogen Passivation of Defects in Multicrystalline Silicon Solar Cells. *Sol. Energy Mater. Sol. Cells* **2003,** *80*, 343-353.

(35) Dautremont-Smith, W. C.; Nabity, J. C.; Swaminathan, V.; Stavola, M.; Chevallier, J.; Tu, C. W.; Pearton, S. J. Passivation of Deep Level Defects in Molecular Beam Epitaxial Gaas by Hydrogen Plasma Exposure. *Appl. Phys. Lett.* **1986,** *49*, 1098-1100.

(36) Rettie, A. J. E.; Chemelewski, W. D.; Emin, D.; Mullins, C. B. Unravelling Small-Polaron Transport in Metal Oxide Photoelectrodes. *J. Phys. Chem. Lett.* **2016,** *7*, 471-479.

(37) Austin, I. G.; Mott, N. F. Polarons in Crystalline and Non-Crystalline Materials. *Adv. Phys.* **1969,** *18*, 41-102.

(38) Zhang, W.; Wu, F.; Li, J.; Yan, D.; Tao, J.; Ping, Y.; Liu, M. Unconventional Relation between Charge Transport and Photocurrent Via Boosting Small Polaron Hopping for Photoelectrochemical Water Splitting. *ACS Energy Lett.* **2018**, 2232-2239.

(39) Abdi, F. F.; Han, L.; Smets, A. H. M.; Zeman, M.; Dam, B.; van de Krol, R. Efficient Solar Water Splitting by Enhanced Charge Separation in a Bismuth Vanadate-Silicon Tandem Photoelectrode. *Nat. Commun.* **2013,** *4*, 2195.

(40) Wrighton, M. S.; Ellis, A. B.; Wolczanski, P. T.; Morse, D. L.; Abrahamson, H. B.; Ginley, D. S. Strontium Titanate Photoelectrodes. Efficient Photoassisted Electrolysis of Water at Zero Applied Potential. *J. Am. Chem. Soc.* **1976,** *98*, 2774-2779.

(41) Benthem, K. v.; Elsässer, C.; French, R. H. Bulk Electronic Structure of $SrTiO_3$: Experiment and Theory. *J. Appl. Phys.* **2001,** *90*, 6156-6164.

(42) Salvador, P.; Gutiérrez, C.; Campet, G.; Hagenmüller, P. Influence of Mechanical Polishing on the Photoelectrochemical Properties of $SrTiO_3$ Polycrystalline Anodes. *J. Electrochem. Soc.* **1984,** *131*, 550-555.

(43) Zhang, W.; Yan, D.; Li, J.; Wu, Q.; Cen, J.; Zhang, L.; Orlov, A.; Xin, H.; Tao, J.; Liu, M. Anomalous Conductivity Tailored by Domain-Boundary Transport in Crystalline Bismuth Vanadate Photoanodes. *Chem. Mater.* **2018,** *30*, 1677-1685.

(44) Eichhorn, J.; Kastl, C.; Cooper, J. K.; Ziegler, D.; Schwartzberg, A. M.; Sharp, I. D.; Toma, F. M. Nanoscale Imaging of Charge Carrier Transport in Water Splitting Photoanodes. *Nat. Commun.* **2018,** *9*, 2597.

(45) Rose, A. Space-Charge-Limited Currents in Solids. *Phys. Rev.* **1955,** *97*, 1538-1544.

(46) Zandi, O.; Klahr, B. M.; Hamann, T. W. Highly Photoactive Ti-Doped α-Fe_2O_3 Thin Film Electrodes: Resurrection of the Dead Layer. *Energy Environ. Sci.* **2013,** *6*, 634-642.

(47) Steier, L.; Herraiz-Cardona, I.; Gimenez, S.; Fabregat-Santiago, F.; Bisquert, J.; Tilley, S. D.; Grätzel, M. Understanding the Role of Underlayers and Overlayers in Thin Film Hematite Photoanodes. *Adv. Funct. Mater.* **2014,** *24*, 7681-7688.

(48) Le Formal, F.; Pendlebury, S. R.; Cornuz, M.; Tilley, S. D.; Grätzel, M.; Durrant, J. R. Back Electron–Hole Recombination in Hematite Photoanodes for Water Splitting. *J. Am. Chem. Soc.* **2014,** *136*, 2564-2574.

(49) Zhang, W.; Yan, D.; Tong, X.; Liu, M. Ultrathin Lutetium Oxide Film as an Epitaxial Hole-Blocking Layer for Crystalline Bismuth Vanadate Water Splitting Photoanodes. *Adv. Funct. Mater.* **2018**, 1705512.

(50) Jang, J.-W.; Du, C.; Ye, Y.; Lin, Y.; Yao, X.; Thorne, J.; Liu, E.; McMahon, G.; Zhu, J.; Javey, A. et al. Enabling Unassisted Solar Water Splitting by Iron Oxide and Silicon. *Nat. Commun.* **2015,** *6*, 7447.

(51) Zhong, D. K.; Choi, S.; Gamelin, D. R. Near-Complete Suppression of Surface Recombination in Solar Photoelectrolysis by "Co-Pi" Catalyst-Modified W:$BiVO_4$. *J. Am. Chem. Soc.* **2011,** *133*, 18370-18377.

(52) Yao, B.; Zhang, J.; Fan, X.; He, J.; Li, Y. Surface Engineering of Nanomaterials for Photo-Electrochemical Water Splitting. *Small* **2019,** *15*, 1803746.

(53) Thorne, J. E.; Jang, J.-W.; Liu, E. Y.; Wang, D. Understanding the Origin of Photoelectrode Performance Enhancement by Probing Surface Kinetics. *Chem. Sci.* **2016,** *7*, 3347-3354.

(54) Barroso, M.; Cowan, A. J.; Pendlebury, S. R.; Grätzel, M.; Klug, D. R.; Durrant, J. R. The Role of Cobalt Phosphate in Enhancing the Photocatalytic Activity of α-Fe_2O_3 toward Water Oxidation. *J. Am. Chem. Soc.* **2011,** *133*, 14868-14871.

(55) Li, W.; He, D.; Sheehan, S. W.; He, Y.; Thorne, J. E.; Yao, X.; Brudvig, G. W.; Wang, D. Comparison of Heterogenized Molecular and Heterogeneous Oxide Catalysts for Photoelectrochemical Water Oxidation. *Energy Environ. Sci.* **2016,** *9*, 1794-1802.

(56) Lin, F.; Boettcher, S. W. Adaptive Semiconductor/Electrocatalyst Junctions in Water-Splitting Photoanodes. *Nat. Mater.* **2013,** *13*, 81.

(57) Laskowski, F. A. L.; Nellist, M. R.; Qiu, J.; Boettcher, S. W. Metal Oxide/(Oxy)Hydroxide Overlayers as Hole Collectors and Oxygen-Evolution Catalysts on Water-Splitting Photoanodes. *J. Am. Chem. Soc.* **2019,** *141*, 1394-1405.

(58) Rettie, A. J. E.; Lee, H. C.; Marshall, L. G.; Lin, J.-F.; Capan, C.; Lindemuth, J.; McCloy, J. S.; Zhou, J.; Bard, A. J.; Mullins, C. B. Combined Charge Carrier Transport and Photoelectrochemical Characterization of $BiVO_4$ Single Crystals: Intrinsic Behavior of a Complex Metal Oxide. *J. Am. Chem. Soc.* **2013,** *135*, 11389-11396.

(59) Nellist, M. R.; Qiu, J.; Laskowski, F. A. L.; Toma, F. M.; Boettcher, S. W. Potential-Sensing Electrochemical AFM Shows CoPi as a Hole Collector and Oxygen Evolution Catalyst on $BiVO_4$ Water-Splitting Photoanodes. *ACS Energy Lett.* **2018,** *3*, 2286-2291.

(60) Cowan, A. J.; Durrant, J. R. Long-Lived Charge Separated States in Nanostructured Semiconductor Photoelectrodes for the Production of Solar Fuels. *Chem. Soc. Rev.* **2013,** *42*, 2281-2293.

(61) Ma, Y.; Kafizas, A.; Pendlebury, S. R.; Le Formal, F.; Durrant, J. R. Photoinduced Absorption Spectroscopy of CoPi on $BiVO_4$: The Function of CoPi During Water Oxidation. *Adv. Funct. Mater.* **2016,** *26*, 4951-4960.

(62) Appavoo, K.; Liu, M.; Black, C. T.; Sfeir, M. Y. Quantifying Bulk and Surface Recombination Processes in Nanostructured Water Splitting Photocatalysts via In Situ Ultrafast Spectroscopy. *Nano Lett.* **2015,** *15*, 1076-1082.

(63) Song, J.; Seo, M. J.; Lee, T. H.; Jo, Y.-R.; Lee, J.; Kim, T. L.; Kim, S.-Y.; Kim, S.-M.; Jeong, S. Y.; An, H. et al. Tailoring Crystallographic Orientations to Substantially Enhance Charge Separation Efficiency in Anisotropic $BiVO_4$ Photoanodes. *ACS Catal.* **2018,** *8*, 5952-5962.

(64) Chen, X.; Liu, L.; Yu, P. Y.; Mao, S. S. Increasing Solar Absorption for Photocatalysis with Black Hydrogenated Titanium Dioxide Nanocrystals. *Science* **2011,** *331*, 746.

(65) Mi, Q.; Ping, Y.; Li, Y.; Cao, B.; Brunschwig, B. S.; Khalifah, P. G.; Galli, G. A.; Gray, H. B.; Lewis, N. S. Thermally Stable N_2-Intercalated WO_3 Photoanodes for Water Oxidation. *J. Am. Chem. Soc.* **2012,** *134*, 18318-18324.

(66) Lichterman, M. F.; Hu, S.; Richter, M. H.; Crumlin, E. J.; Axnanda, S.; Favaro, M.; Drisdell, W.; Hussain, Z.; Mayer, T.; Brunschwig, B. S. et al. Direct Observation of the Energetics at a Semiconductor/Liquid Junction by Operando X-Ray Photoelectron Spectroscopy. *Energy Environ. Sci.* **2015,** *8*, 2409-2416.

(67) Zandi, O.; Hamann, T. W. Determination of Photoelectrochemical Water Oxidation Intermediates on Haematite Electrode Surfaces Using Operando Infrared Spectroscopy. *Nat. Chem.* **2016,** *8*, 778.

(68) Fabbri, E.; Abbott, D. F.; Nachtegaal, M.; Schmidt, T. J. Operando X-Ray Absorption Spectroscopy: A Powerful Tool toward Water Splitting Catalyst Development. *Curr. Opin. Electrochem.* **2017,** *5*, 20-26.

(69) Toma, F. M.; Cooper, J. K.; Kunzelmann, V.; McDowell, M. T.; Yu, J.; Larson, D. M.; Borys, N. J.; Abelyan, C.; Beeman, J. W.; Yu, K. M. et al. Mechanistic Insights into Chemical and Photochemical Transformations of Bismuth Vanadate Photoanodes. *Nat. Commun.* **2016,** *7*, 12012.

(70) Higashi, M.; Domen, K.; Abe, R. Highly Stable Water Splitting on Oxynitride TaON Photoanode System under Visible Light Irradiation. *J. Am. Chem. Soc.* **2012,** *134*, 6968-6971.

(71) Ohno, T.; Bai, L.; Hisatomi, T.; Maeda, K.; Domen, K. Photocatalytic Water Splitting Using Modified GaN:ZnO Solid Solution under Visible Light: Long-Time Operation and Regeneration of Activity. *J. Am. Chem. Soc.* **2012,** *134*, 8254-8259.

(72) Su, J.; Wei, Y.; Vayssieres, L. Stability and Performance of Sulfide-, Nitride-, and Phosphide-Based Electrodes for Photocatalytic Solar Water Splitting. J. *Phys. Chem. Lett.* **2017,** *8*, 5228-5238.

(73) Castelli, I. E.; Hüser, F.; Pandey, M.; Li, H.; Thygesen, K. S.; Seger, B.; Jain, A.; Persson, K. A.; Ceder, G.; Jacobsen, K. W. New Light-Harvesting Materials Using Accurate and Efficient Bandgap Calculations. *Adv. Energy Mater.* **2015,** *5*, 1400915.

(74) Curtarolo, S.; Hart, G. L. W.; Nardelli, M. B.; Mingo, N.; Sanvito, S.; Levy, O. The High-Throughput Highway to Computational Materials Design. *Nat. Mater.* **2013,** *12*, 191.

Figures

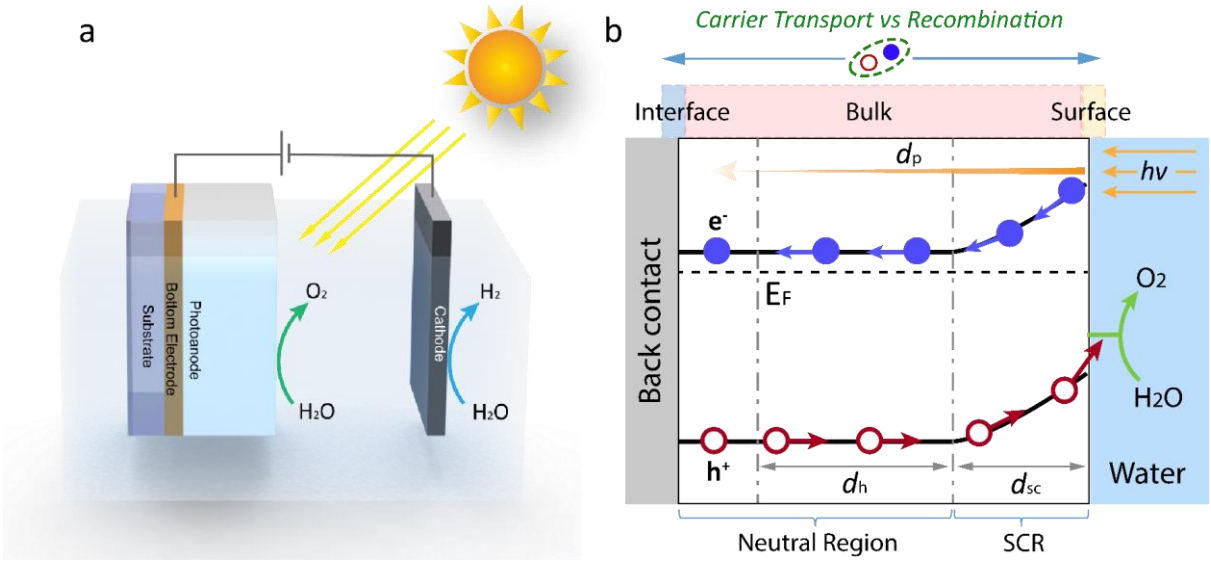

Figure 1 (a) Schematic of a thin film photoanode for PEC water splitting. (b) Schematic of photocarrier generation, transport and recombination across a semiconductor photoanode, including bulk, surface and interface. Representative regions for the photoanode design are highlighted by the space charge region thickness (d_{sc}), minority carrier diffusion length (d_h) and effective photon attenuation depth (d_p).

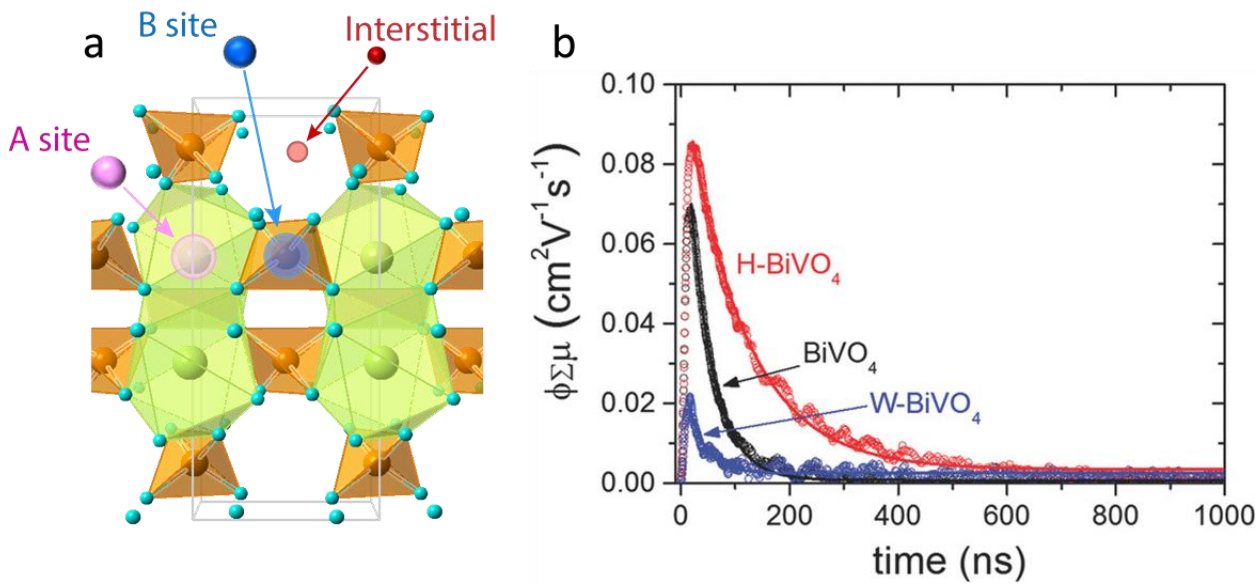

Figure 2 (a) Substitutional (A-site and B-site) and interstitial doping in the BVO model system. (b) Time-resolved microwave conductivity plots for pristine, hydrogen-annealed, and W-doped BVO films demonstrating the impact of different dopants on carrier dynamics. Reprinted with permission from ref 33. Copyright 2017 Wiley.

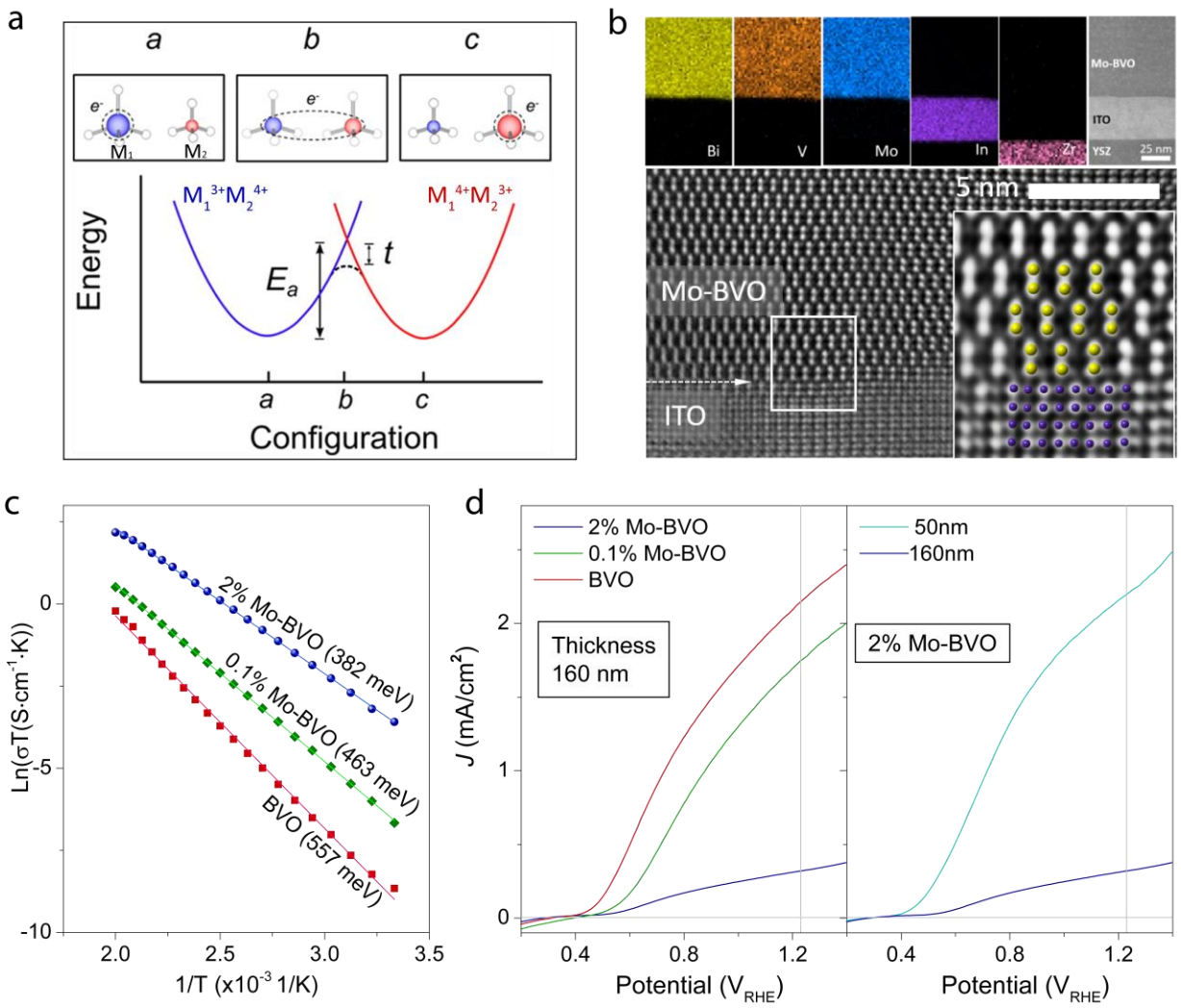

Figure 3. (a) Schematic of small polaron transport. The strong electron-lattice interaction applies an energy barrier (E_a) for the electron transfer between neighboring lattice units. Reprinted with permission from ref 36. Copyright 2016 American Chemical Society. (b) Cross-sectional EDX mapping and the atomic-resolution STEM image demonstrate phase-pure and single-crystalline growth of Mo-BVO thin films over single-crystalline ITO/YSZ substrates. (c) Thin film conductivity-temperature fitting plots of Mo-BVO films for linear extrapolation of the small polaron hopping barrier. (d) Photocurrent density versus potential (*J*-*V*) curves of 160-nm-thick Mo-BVO films with different doping levels (left panel) and 2% Mo-BVO film with different thicknesses (right panel) measured under back illumination for sulfite oxidation (pH 7.0, 1M Na_2SO_3). Reprinted with permission from ref 38. Copyright 2018 American Chemical Society.

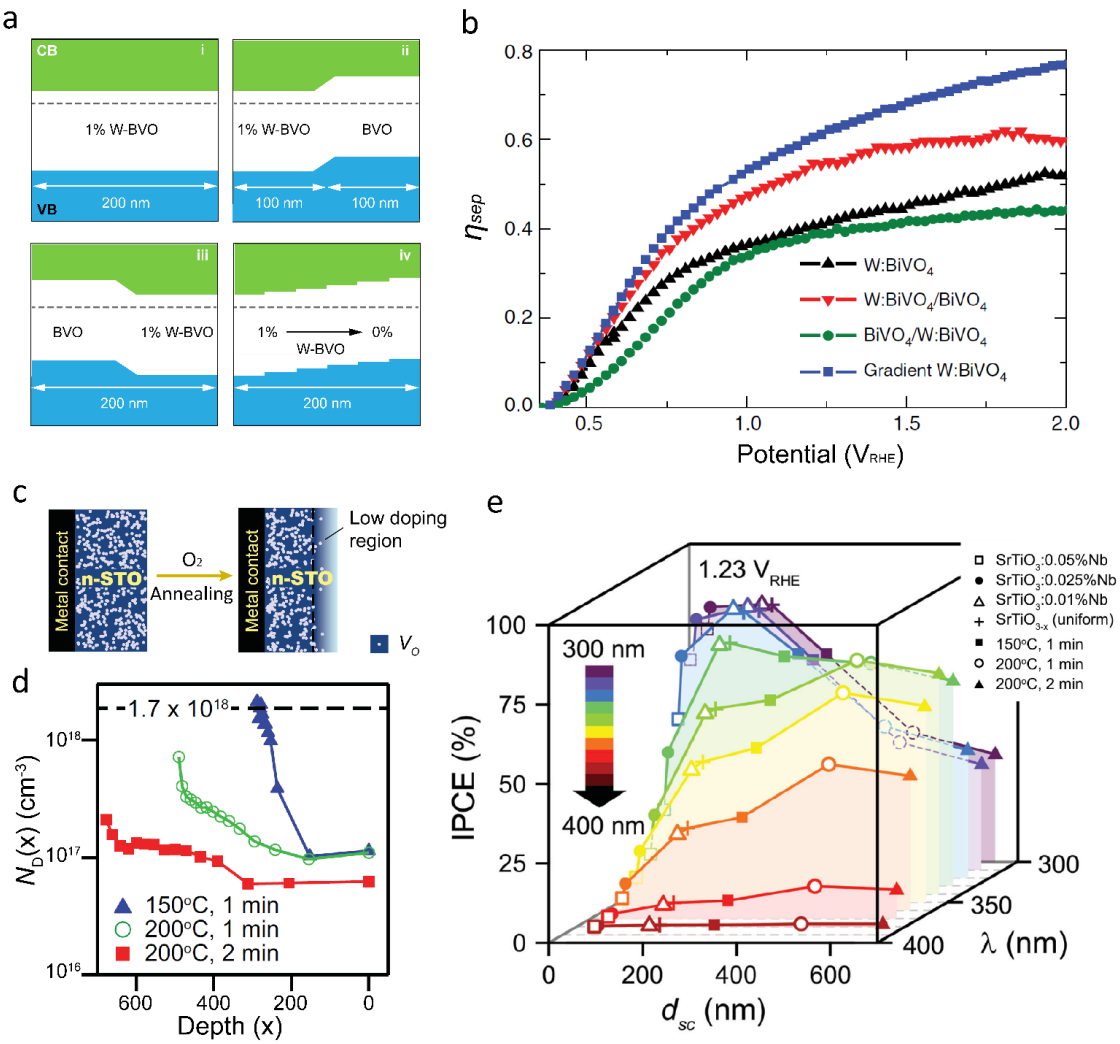

Figure 4. (a) Schematic of the band diagram of (i) 1% W-doped BVO, (ii) W-doped BVO/BVO homojunction, (iii) reversed W-doped BVO/BVO homojunction, and (iv) graded W-doped BVO/BVO homojunction. (b) Charge carrier separation efficiency (η_{sep}) as a function of external potential (V_{RHE}) for the above junctions. Reprinted with permission from ref 39. Copyright 2013 Nature Publishing Group. (c) Schematic of creating a gradient doping region over *n*-STO through refilling the oxygen vacancies via rapid thermal reoxidation. (d) Donor density (N_D) as a function of depth *x* for *n*-STO photoanodes under different reoxidation conditions, as determined from the Mott-Schottky analysis. The depth *x* is the distance from the semiconductor top surface. (e) IPCE values at 1.23 V_{RHE} as a function of respective space charge region width and incident light wavelength for *n*-STO photoanodes under different thermal annealing conditions. Each type of symbols represents the data collected from the same sample. Reprinted with permission from ref 16. Copyright 2016 Wiley.

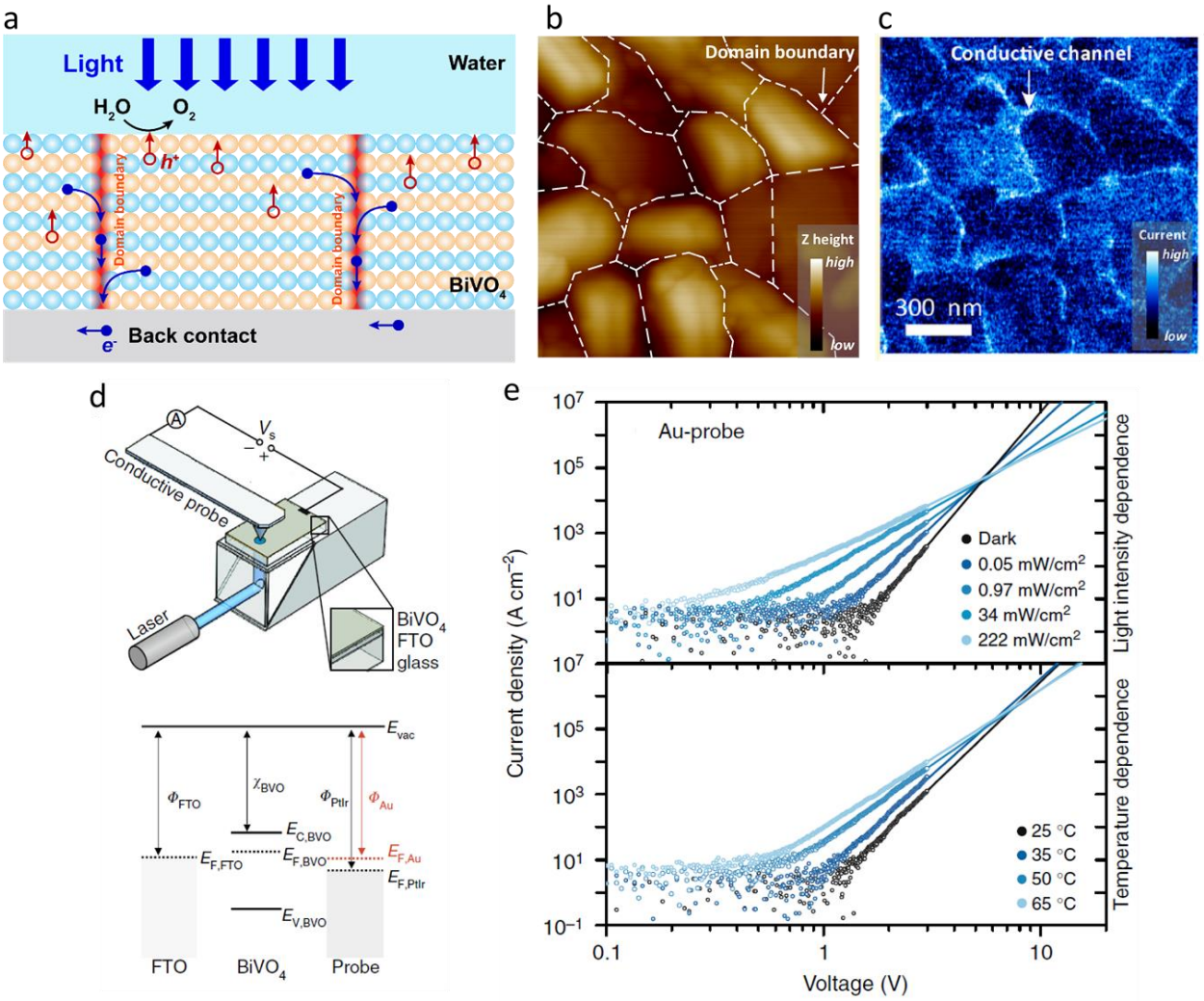

Figure 5. (a) Schematic of domain-boundary conduction on improving carrier transport in the intrinsically insulating BVO. (b) Topography z-height atomic force microscope (AFM) image and (c) simultaneously acquired conductive AFM image of the c-axis oriented BVO films grown on single-crystalline ITO/YSZ substrates. The domain boundaries are highlighted by white dashed lines in b. Reprinted with permission from ref 43. Copyright 2018 American Chemical Society. (d) The upper schematic shows the photoconductive atomic force microscope (pc-AFM) setup. The illumination is provided thought the substrate side. Two types of conductive coatings, e.g. Au and PtIr, are used on the AFM probes to study the effect of different metal-semiconductor contacts on the photocurrent output. The lower schematic shows the energy band diagram between FTO, BVO and the probe coating metals. (e) Illumination and temperature dependence of solid-state current-voltage characteristics for Au-probe/BVO/FTO junctions. Reprinted with permission from ref 44. Copyright 2013 Nature Publishing Group.

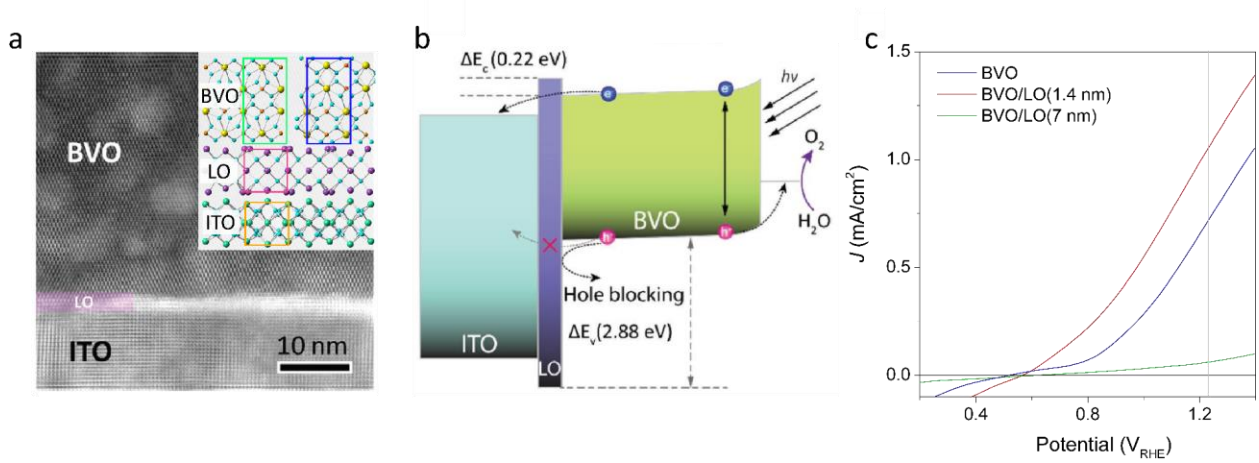

Figure 6. (a) High-resolution STEM image near the BVO/LO/ITO region demonstrating the ultrathin epitaxial LO interlayer and the epitaxial BVO film growth. Inset shows the crystallographic mode demonstrating the epitaxial relation between BVO, LO and ITO. (b) Schematic energy-band diagram of BVO/LO/ITO with valence band maximum (VBM) and conduction band minimum (CBM). The ultrathin LO interlayer drives hole delivery to the semiconductor–electrolyte interface through the hole-blocking effect. (c) *J-V* curves of the BVO/LO thin film photoanodes with different LO layer thicknesses. Reprinted with permission from ref 49. Copyright 2018 Wiley.

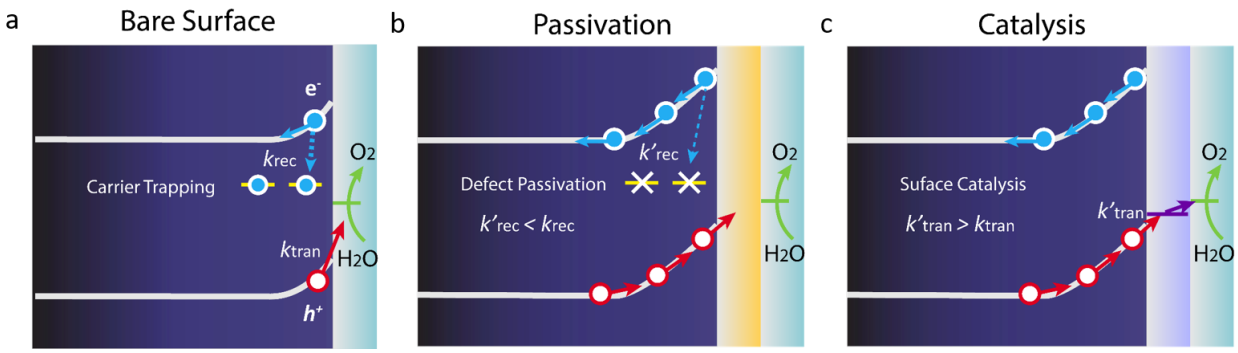

Figure 7. Schematic of surface defect engineering by passivation and catalysis. The carrier transport efficiency near the surface can be improved by lowering the recombination rate k_{rec} (defect passivation) or improving the transfer rate k_{tran} (surface catalysis).

Quotes to highlight in paper

1. Carrier transport in semiconductor photoelectrodes is a key process that determines the PEC device efficiency and is extremely sensitive to the materials defect level.

2. Although the uniform bulk doping using hydrogen or hexavalent ions apparently improves the PEC performance, the fundamental mechanism has yet to be fully elucidated.

3. Instead of introducing a homogeneous spatial profile of dopants, graded doping artificially constructs a sloped or stepped distribution of the doping level to form distributed homo-junctions.

4. Beside tuning the intrinsic materials characteristics with bulk defect, engineering extrinsic structural imperfections, such as mobile charged defects at boundaries, is effective to improve carrier transport.

5. To facilitate carrier transfer across the back contact, careful interface design is required in terms of structural, chemical and electronic matching.

6. These defect engineering strategies are not isolated from each other and may work together to improve the photoelectrode performance.